CHAPTER

4

The Contribution of Human Superior Intraparietal Sulcus to Visual Short-Term Memory and Perception

Yaoda Xu, Su Keun Jeong
Harvard University, Cambridge, MA, USA

INTRODUCTION

Visual short-term memory (VSTM) is a short-term memory buffer that temporarily stores visual information (Phillips, 1974). It has a durable but very limited capacity (Luck & Vogel, 1997; Pashler, 1988; Phillips, 1974). Although VSTM has often been studied in isolation, it is an integral part of visual perception (Xu, 2002). This is because, theoretically, it would not be possible to separate perception from VSTM, because for perception to occur, visual information has to be encoded in some kind of short-term memory buffer before further processing can take place. In practice, the paradigms employed to study perception often ask observers to report a briefly presented visual stimulus, necessarily engaging VSTM, making any results obtained a reflection of both sensory processing and VSTM characteristics. In cognitive neuroscience research, the brain areas engaged in sensory processing are found to also participate in VSTM information maintenance (e.g., Harrison & Tong, 2009; Xu & Chun, 2006). As such, VSTM is tightly integrated with visual perception.

In everyday visual perception, we are often faced with a huge number of visual inputs, some being essential to task performance and some being just pure distractions. To ensure proper task performance, it is critical that our visual system selectively retains and processes what is most relevant to the current goals and thoughts of the observer. As such, by examining what is stored in VSTM and the control process that determines what is stored there, we can gain an in-depth understanding of how goal-directed visual perception is accomplished. VSTM is therefore not an isolated cognitive operation. But rather, understanding the characteristics of VSTM will provide us with better knowledge of how visual perception works in general.

Over the years, researchers have attempted to understand what limits VSTM capacity. Although some have proposed a slot-like representation in which a fixed number of about three or four visual objects can be represented in VSTM (Cowan, 2001; Luck & Vogel, 1997; Vogel, Woodman, & Luck, 2001; Zhang & Luck, 2008), others have argued instead that its resources can be flexibly divided among objects and, depending on the encoding demands, information from more than three or four objects may be represented in VSTM (Alvarez & Cavanagh, 2004; Bays & Husain, 2008; van den Berg, Shin, Chou, George, & Ma, 2012; Wilken & Ma, 2004). As supporting experimental evidence exists for both accounts, it seems that neither account alone can fully accommodate all the experimental findings, how should we then understand what determines VSTM capacity limit?

The human brain has evolved to accommodate the demands of information processing within. As such, examining brain activation associated with a particular task can provide us with vital clues about the processing algorithm employed in accomplishing the task. Prior neuroimaging research has identified a brain region in human intraparietal sulcus (IPS) that tracks the number of items stored in VSTM (Todd & Marois, 2004, 2005; see also a related event-related brain potential finding from Vogel & Machizawa, 2004). The discovery of this neural substrate provided a unique opportunity for us to

http://dx.doi.org/10.1016/B978-0-12-801371-7.00004-1

understand whether slots or flexible resources would best characterize information representation in VSTM. By manipulating the complexity of the visual objects encoded and thereby the encoding demands of each object, Xu and Chun (2006) found that although a region in the inferior IPS tracks a fixed number of about four objects regardless of object complexity, a region in superior IPS (corresponding to the IPS area identified by Todd & Marois, 2004) tracked the number of objects successfully retained in VSTM, which was variable depending on the encoding demands of each object. Consistent with this functional magnetic resonance imaging (fMRI) finding, a recent event-related brain potential study reported that electrodes at different sites showed dissociable effects corresponding to both the slot-like and the flexible resource-based representations in VSTM (Wilson, Adamo, Barense, & Ferber, 2012). Thus, both types of representations can play a role in VSTM information representation, with slot-like representation involved in object selection and flexible resource-based representation involved in the encoding and retention of information in VSTM.

Based on this initial neuroimaging result and subsequent findings (Xu, 2007, 2008, 2009; Xu & Chun, 2006, 2007) and existing ideas and results from behavioral studies, Xu and Chun (2009) proposed the neural object file theory and argued that there exists two distinctive stages of visual information processing whenever multiple visual objects need to be selected and encoded. The first stage is object individuation and involves the inferior IPS. Here a fixed number of about four objects from a crowded scene are selected based on their spatial information. The second stage is object identification and involves superior IPS and higher visual areas. Here details of the selected objects are encoded and retained. This theory not only resolves the debate regarding what determines VSTM capacity limit, but also accounts for a number of other (sometimes puzzling) behavioral results, such as those obtained in multiple visual object tracking in which observers failed to detect obvious feature changes on successfully attended and tracked objects (Bahrami, 2003). The neural object file theory also bridges studies on object perception in humans after parietal brain lesion (Coslett & Saffran, 1991) and the development of object concepts in infants (Leslie, Xu, Tremoulet, & Scholl, 1998) (for details of how the neural object file theory accounts for all of these, see Xu & Chun, 2009).

The involvement of superior IPS in VSTM information encoding and retention suggests that this brain region can represent a variety of visual information dynamically based on the task demands. This echoes findings from monkey neurophysiological studies in which neurons in lateral intraparietal (LIP) sulcus have been shown to dynamically encode behaviorally relevant visual stimuli (Gottlieb, Kusunoki, & Goldberg, 1998; Toth & Assad, 2002). Meanwhile, existing neuropsychological and neuroimaging studies have associated human parietal cortex primarily with attention-related processing (Corbetta & Shulman, 2002; Szczepanski, Konen, & Kastner, 2010; Wojciulik & Kanwisher, 1999; Yantis et al., 2002). As such, although Xu and Chun (2009) imply that information can be directly represented in IPS during visual processing, it is also possible that parietal activation simply tracks the deployment of attentional resources without actually carrying detailed visual representations.

Recent development in fMRI multivoxel pattern analysis (MVPA) has enabled researchers to decode fMRI response patterns and gain a better understanding of the nature of information representation in specific brain regions (Cox & Savoy, 2003; Haxby et al., 2001; Haynes & Rees, 2006; Norman, Polyn, Detre, & Haxby, 2006; Peelen & Downing, 2007). Using this approach, here we aim to understand whether the content of VSTM could be successfully decoded from fMRI response patterns in the superior IPS or whether superior IPS response patterns are oblivious to what is stored in VSTM. We were able to successfully decode object information in the superior IPS, showing that visual information can be directly represented in the superior IPS. Importantly, this representation is task dependent and reflects the encoding of visual information that is needed for the successful performance of the current task. These results are thus consistent with those obtained from fMRI response amplitude measures (e.g., Todd & Marois, 2004; Xu & Chun, 2006) and support the notion that the superior IPS likely plays a key role in mediating the moment-to-moment, goal-directed visual information representation in the human brain.

MATERIALS AND METHODS

Participants

Five observers (3 females, mean age = 31.8 years, standard deviation = 1.92) participated in Experiments 1 and 2, with at least a two-month separation. One additional observer (1 male) participated in Experiment 2 in an effort to see whether adding more observers would change the results of Experiment 2 in any substantial way (which it did not). Because this observer then left the area and was unable to come back to participate in Experiment 1, his data from Experiment 2 were excluded from the final analyses. One more observer was scanned in Experiment 2, but excluded from data analysis because of excessive head motion (greater than 5 mm). In Experiment 2, two observers' behavioral data for the main experiment were not recorded because of equipment failure.

All observers had normal, or corrected-to-normal, visual acuity and reported no history of neurological impairment. They were recruited from the Harvard University community and received payments for their participation in the experiments. All observers gave their informed consent before their participation in the experiment. The study was approved by the institutional review board of Harvard University.

Experimental Design

Main Experiments

During both Experiments 1 and 2, observers viewed a sequential presentation of 10 unique object images either all above or all below the central fixation dot (see Figure 1). The 10 images were drawn from the same object category and shared the same general shape contour (e.g., 10 side-view shoe images, see Figure 1). Different shape categories were viewed in different trial blocks. In Experiment 1, observers viewed the images and detected an immediate repetition of the same image (one-back task), requiring them to store each image in VSTM. In Experiment 2, instead of the one-back task, observers viewed the images and detected the direction of object motion that occurred randomly twice in each block of trials, making neither object shape nor location task relevant.

Two square-shaped white placeholders were present above and below the central fixation during each block to mark the two object locations. The white placeholders subtended 7.0° × 4.7°, with the distance between the fixation and the center of each placeholder being 3.2°. Each object exemplar subtended approximately 5.5° × 2.8°. Each stimulus block lasted 8 s and contained 10 unique images, with each image appearing for 300 ms followed by a 500 ms blank display. Fixation blocks, lasting 8 s, were inserted at the beginning and end of the run, as well as between adjacent stimulus blocks. The presentation order of the different stimulus blocks and that of the images within each block were chosen randomly for each run.

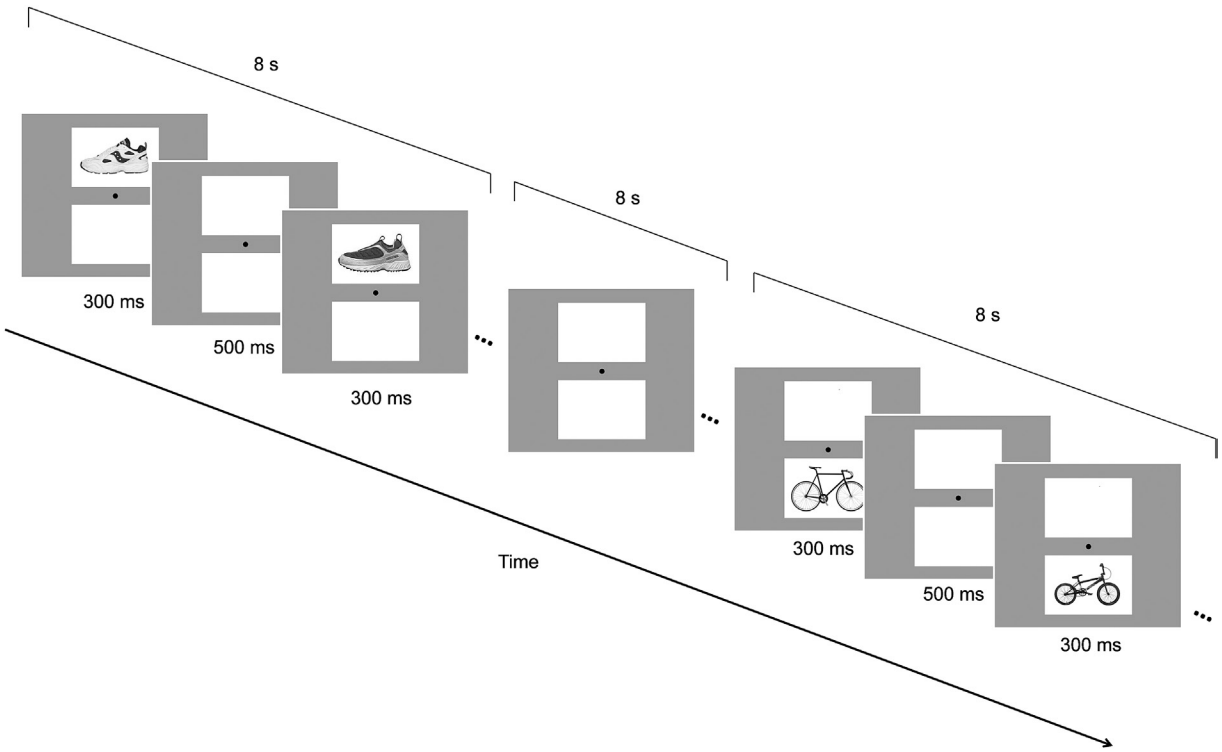

FIGURE 1 Example stimuli and trial structure. In both Experiments 1 and 2, observers viewed a sequential presentation of 10 unique object images either all above or all below the central fixation dot. The 10 images were drawn from the same object category and shared the same general shape contour. Different shape categories were viewed in different trial blocks. In Experiment 1, observers viewed the images and detected an immediate repetition of the same image, making object shape, but not location, task-relevant. In Experiment 2, observers passively viewed the images and detected the direction of an occasional image jitter (either horizontal or vertical), making neither object shape nor location task relevant.

In Experiment 1, two object categories were used, namely shoe and bike. Each run contained three blocks of trials for each category at each location. Each observer was tested with six runs, each lasting 3 min 28 s. Thus, for each observer, a total of 72 blocks were collected with 18 blocks for each object category at each of the two locations.

In Experiment 2, four object categories were used, namely shoe, bike, guitar, and couch. Each stimulus block appeared once in each run. There were also stimulus conditions in which two objects appeared simultaneously with one above and one below the fixation. These conditions were intended for a different study and were excluded from the present analysis. Each observer had 8 to 10 runs, each lasting 5 min 36 s. Thus, for each observer, a total of 64–80 blocks were collected with 8–10 blocks for each object category at each of the two locations.

Superior IPS Localizer

To localize superior IPS, following previous studies (Todd & Marois, 2004; Xu & Chun, 2006), we conducted an object VSTM experiment. Observers were asked to remember which object category was shown at which location and to judge whether the probe object (a new object) shown in the test display matched the category of the object shown at the same location in the sample display. A given sample display contained one to four unique objects appearing in four possible locations around the central fixation, with each object being an exemplar from a different category. The four possible object locations were located above, below, or to the right or left of the central fixation. These locations were marked with white placeholders visible throughout the trial. For no-change trials, the probe object in the test display would match the object category shown at the same location in the sample display but would be a different exemplar from the same category; and for change trials, the probe object would be an exemplar from a different category. Gray-scale photographs of everyday objects from four categories (shoes, bikes, guitars, and couches) were used as stimuli.

Each trial lasted 6 s and included a fixation period (1000 ms), a sample display (200 ms), a delay period (1000 ms), a test display/response period (2500 ms), and a feedback (1300 ms). The display subtended approximately 12° × 12°, with the distance between the fixation and the center of each object being 4° and the size of the placeholder being 4.5° × 3.6°. With a counterbalanced trial history design, each run contained 15 stimulus trials for each set size and 15 fixation trials in which only the central fixation dot appeared for 6 s. Three filler trials were added for practice and trial history balancing purposes (two at the beginning and one at the end of the run), but were excluded from data analysis. Each observer was tested with two runs, each lasting 8 min.

Inferior IPS/Lateral Occipital (LO) Localizer

Following previous studies (Xu & Chun, 2006, 2007; Xu, 2007, 2008, 2009), observers viewed blocks of objects and noise images. The object images were the set size four displays from the superior IPS localizer. For the noise images, we took the object images but phase-scrambled each component object. Each block lasted 16 s and contained 20 images, each appearing for 500 ms followed by a 300-ms blank display. Observers were asked to detect the direction of a slight spatial jitter (either horizontal or vertical), which occurred randomly once in every 10 images. Each run contained eight object blocks and eight noise blocks. Each observer was tested with two or three runs, each lasting 4 min 40 s.

To ensure proper fixation, we monitored observers' eye movement in the main experiments by using an EyeLink 1000 eye tracker.

fMRI Methods

fMRI data were acquired from a Siemens Tim Trio 3T scanner. Observers viewed images back projected onto a screen at the rear of the scanner bore through an angled mirror mounted on the head coil. All experiments were controlled by an Apple MacBook Pro running Matlab with Psychtoolbox extensions (Brainard, 1997). For anatomical images, high-resolution 144 T1-weighted images were acquired (echo time, 1.54 ms; flip angle, 7°; matrix size, 256 × 256; repetition time, 2200 ms; voxel size, 1 × 1 × 1 mm). For the functional images, T2*-weighted echo-planar gradient echo sequence was used (Huettel, Song, & McCarthy, 2009). For the two main experiments and the inferior IPS/lateral occipital (LO) localizer runs, 31 near axial slices (3 × 3 mm in plane, 3 mm thick, 0 skip, interleaved acquisition) were acquired (echo time, 30 ms; flip angle, 90°; matrix size, 72 × 72; repetition time, 2000 ms). The number of volumes collected for Experiment 1, Experiment 2, and the inferior IPS/LO localizer runs were 168, 104, and 140, respectively. For superior IPS localizer runs, 24 slices (3 × 3 mm in plane, 5 mm thick, 0 skip) parallel to the AC-PC line were acquired (volumes, 320; echo time, 29 ms; flip angle, 90°; matrix size, 72 × 72; repetition time, 1500 ms).

Data Analysis

fMRI data were analyzed in native space with BrainVoyager QX (http://www.brainvoyager.com). Data preprocessing included three-dimensional motion correction, slice acquisition time correction, linear trend removal, and the removal of the first two volumes of each functional run. No spatial smoothing or other data preprocessing was applied.

fMRI data from the localizer runs were analyzed using general linear models. All regions of interest (ROIs) were defined separately in each individual observer. Following previously established procedures (Xu & Chun, 2006), LO and inferior IPS ROIs were defined as voxels showing higher activations to the object than to the noise displays (false discovery rate (FDR) $q < 0.05$, corrected for serial correlation) in lateral occipital cortex and the inferior part of the IPS bordering the traverse occipital sulcus, respectively. As was done before (Todd & Marois, 2004; Xu & Chun, 2006), superior IPS was defined as voxels tracking each observer's behavioral VSTM capacity. This was achieved by first calculating each observer's behavioral VSTM capacity based on Cowan's K formula (Cowan, 2001), and then in a multiple regression analysis weighing the regression coefficient for each set size with that observer's behavioral VSTM capacity for that set size. Superior IPS was defined as voxels showing significant activations in the regression analysis (FDR $q < 0.05$, corrected for serial correlation).

During MVPA analysis, for each observer, we overlaid the ROIs onto the raw fMRI data from the main experiments, applied a general linear model to the data, and extracted the resulting beta-weights for each stimulus condition in each voxel of each ROI. These beta-weights then served as the input to our MVPA analysis. Following Haxby et al. (2001), we first divided the input data into odd and even runs and then normalized the data within each ROI by removing the mean across all stimulus conditions. This normalization procedure was carried out based on the assumption that the neural response pattern for each stimulus condition is a linear combination of the shared pattern across all conditions and a distinctive pattern unique to that condition. As such, subtracting the mean response would eliminate the contribution of the shared pattern and amplify neural pattern differences among the different stimulus conditions. This normalization method could result in negative correlation between conditions. But because the main dependent variable of interest is the relative differences between correlations rather than the absolute values of the correlations themselves, this normalization procedure provides a good way to illustrate the results and has been used successfully in previous studies (Haxby et al., 2001; Schwarzlose, Swisher, Dang, & Kanwisher, 2008). Because this normalization procedure may distort results when the number of stimulus conditions is small (Garrido, Vaziri-Pashkam, Nakayama, & Wilmer, 2013), we also analyzed data without normalization and with z-scoring to remove amplitude differences among the different conditions. Both analyses revealed similar results as those obtained with the normalization procedure.

To decode the nature of representation contained in each ROI, we correlated voxel response patterns from odd runs with those from even runs across all stimulus condition pairs. This resulted in four correlation conditions: both same (same location and same shape pairs), location change (same shape and different location pairs), shape change (different shape and same location pairs), and both change (different shape and different location pairs). The resulting correlation coefficients were Fisher-transformed to ensure normal distribution of the values and then subjected to a repeated-measures analysis of variance with shape (same, different) and location (same, different) as factors. To directly show shape and location representation in each ROI, we also obtained the main effect of shape by calculating the difference between conditions that shared the same shape and those that did not, averaging over both the location same and change conditions. Similarly, we obtained the main effect of location by calculating the difference between conditions that shared the same location and those that did not, averaging over both the shape same and change conditions.

RESULTS

In Experiment 1, while undergoing an fMRI scan, observers viewed a sequential presentation of 10 unique object images either all above or all below the central fixation dot (see Figure 1). The 10 images were drawn from the same object category and shared the same general shape contour (e.g., 10 side-view shoe images, see Figure 1). Different shape categories (shoes and bikes) were viewed in different trial blocks. Observers viewed the images and detected an immediate repetition of the same image, requiring them to store each image in VSTM. Object shape, but not location, was thus task-relevant. Observers were fairly accurate in detecting shape repetitions and had an average behavioral accuracy of 88.40 ± 6.10%.

To examine information representations in a brain region, following Haxby and colleagues (Haxby et al., 2001), after normalizing fMRI response amplitudes to the mean of all the stimulus conditions, we calculated correlation coefficient between fMRI response patterns from odd and even runs (see Methods). If a brain region contains distinct neural representations resulting in distinct fMRI response patterns for different object shapes, then higher correlation coefficients of

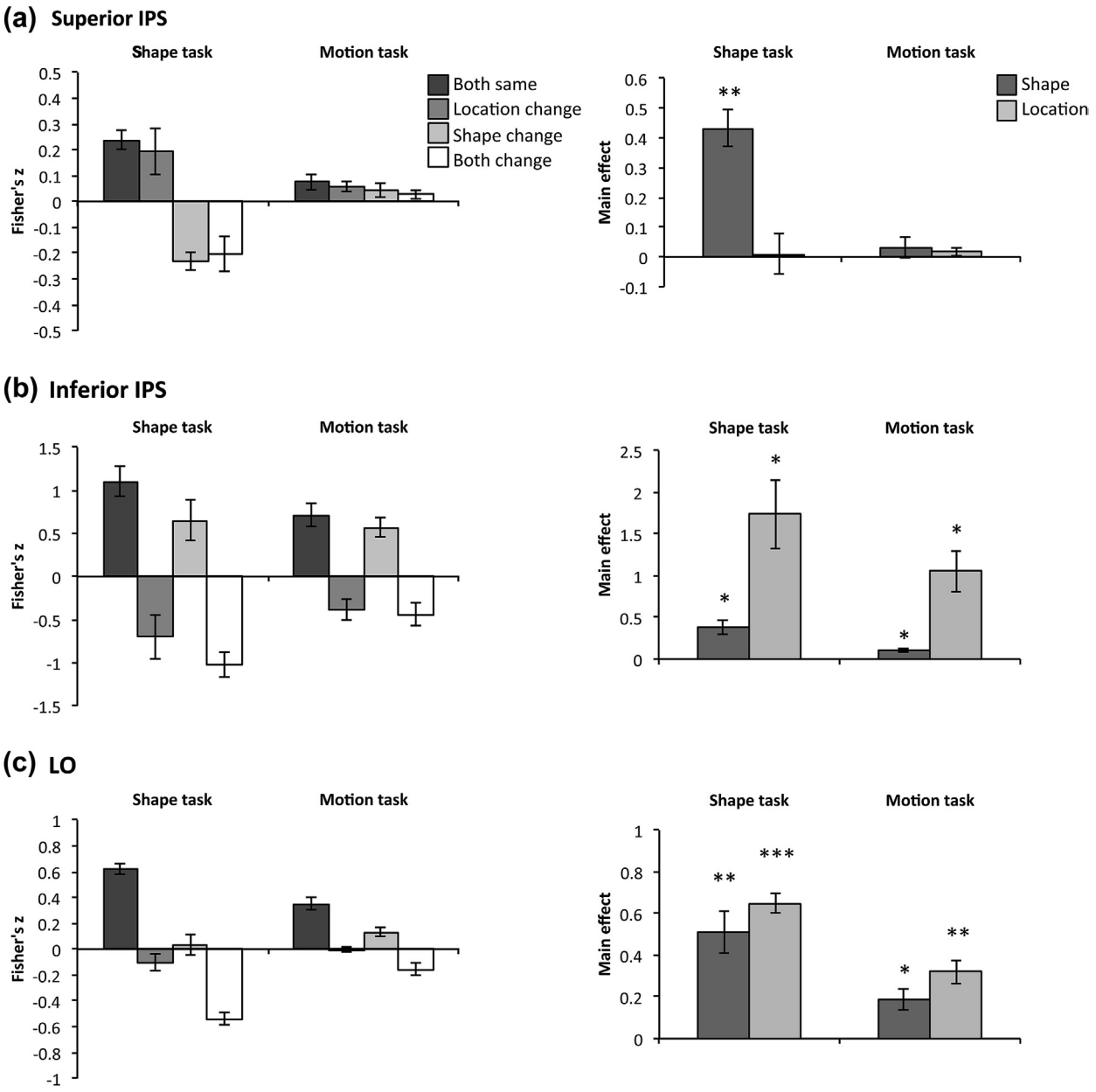

FIGURE 2 (Left column) Results from Experiments 1 and 2 showing Fisher-transformed correlation coefficients of functional magnetic resonance imaging response pattern correlations (i.e., decoding) between pairs of stimulus conditions from odd and even runs. Each pair could share both shape and location (both), shape but not location (location change), location but not shape (shape change), or neither features (both change). (Right column) Main effects of shape and location decoding in Experiments 1 and 2(a)–(c) Results for the superior intraparietal sulcus (IPS), inferior IPS, and lateral occipital (LO), respectively. In the superior IPS, shape decoding was observed in Experiment 1 but not in Experiment 2. No location decoding was observed in either experiments. In the LO and inferior IPS, shape and location decoding was observed in both experiments with decoding being more robust in Experiment 1 than 2. In the left column, black, dark gray, light gray, and white bars indicate correlation coefficients for "Both Same," "Location Change," "Shape Change," and "Both Change" pairs, respectively. In the right column, dark gray and light gray bars indicate main effect of shape and location, respectively. Error bars indicate within-subject standard error of the mean. *$p < .05$; **$p < .01$; ***$p < .001$.

fMRI response patterns would be expected when the same than different object shapes were shown in odd and even runs. Likewise, if spatial locations (i.e., above and below fixation) are uniquely represented in a brain region, then higher correlation coefficients should be observed when objects appeared in the same than in different locations in odd and even runs.

In superior IPS, successful decoding emerged for object shapes, with the correlation coefficient being higher between the same than different shapes shown in odd and even runs ($F_{1,4} = 50.80$, $p = .002$; see Figure 2(a)). This indicates that superior IPS carries the content of VSTM. Such decoding success, however, was absent for object locations ($F < 1$,

$p > .89$). The interaction between shape and location decoding was not significant ($F < 0.19$, $p > .68$), showing that shape decoding was not modulated by whether shapes appeared in the same or different locations.

To understand whether shape representation in superior IPS is task-dependent, in Experiment 2, we repeated the design of Experiment 1, but asked the same group of observers from Experiment 1 to passively view the images and detected the direction of an occasional image jitter (either horizontal or vertical). This task requirement made neither object shape nor location task-relevant. To ensure that our result from Experiment 1 was not due to the two unique object categories (shoes and bikes) selected, in addition to shoes and bikes, we also included guitars and couches in Experiment 2 (see Methods). There were no main decoding difference between shoes and bikes and between guitars and couches ($F < 1$, $p > .90$) and no interaction between the two object groups and shape or location decoding ($F < 1$, $p > .52$). As such, results from all four categories were combined in Experiment 2.

Overall, observers were again fairly accurate in their behavioral performance (93.68 ± 5.75%). In superior IPS, no decoding of either shape or location was obtained (no main effects of shape and location, $F < 1.57$, $p > .28$; see Figure 2(a)). Direct comparison between the two experiments revealed shape decoding by experiment interaction ($F_{1,4} = 24.25$, $p = .008$), but not location decoding by experiment interaction ($F < 1$, $p > .90$). These results were not influenced by minor design differences between the two experiments. When we only included the same number of shoes/bikes trials from the two experiments, despite a reduction of power, shape decoding was still present in Experiment 1 ($F_{1,4} = 8.86$, $p = .041$), but absent in Experiment 2 ($F_{1,4} < 1$, $p > .55$), with an almost significant interaction between shape decoding and experiment ($F_{1,4} = 4.52$, $p = .06$). As before, location decoding never reached significance in either experiments in this analysis ($Fs < 2.48$, $ps > .19$). Thus, superior IPS carries shape representation, but only when such information was required by the task.

To determine whether task-dependent object shape representation seen in superior IPS is present in other brain regions involved in visual object representation, we also examined responses in the LO and another parietal region, the inferior IPS. The LO plays an important role in visual object shape representation and damage to it can lead to severe deficits in object shape perception (Milner et al., 1991). Consistent with this neuropsychological finding, both fMRI response amplitudes and patterns from the LO have been correlated with success in object shape identification (Grill-Spector, Kushnir, Hendler, & Malach, 2000; Williams, Dang, & Kanwisher, 2007). Interestingly, recent studies have also shown that both object shape and location can be decoded from this brain region (Kravitz, Kriegeskorte, & Baker, 2010; Schwarzlose, et al., 2008). As mentioned previously, the inferior IPS has previously been shown to participate in object selection and individuation via location and may contain coarse object shape information necessary for carrying out these operations (Jeong & Xu, 2013; Xu & Chun, 2006, 2009).

To examine shape and location encoding in the LO and inferior IPS, to increase power, we first combined data from all categories from Experiment 2 in our analyses. Consistent with prior findings, in both experiments, object shape and location information could be reliably decoded in both the inferior IPS and LO (Figure 2(b) and 2(c), $Fs > 14.42$, $ps < .019$). In Experiment 1, shape and location decoding did not interact in either the LO or inferior IPS ($Fs < 2.42$, $ps > .19$). In Experiment 2, shape and location did not interact in the LO ($F < 1.23$, $p > .32$) but had a marginally significant interaction in the inferior IPS ($F_{1,4} = 7.4$, $p = .053$). These results show that, regardless of the task demands, both shape and location could be decoded in LO and inferior IPS, with shape and location encoding being largely independent of each other. Direct comparison between experiments revealed a shape by experiment interaction ($Fs > 9.49$, $ps < .037$) in both inferior IPS and LO. Location by experiment interaction was also significant in LO ($F_{1,4} = 14.90$, $p = .018$) and marginally significant in inferior IPS ($F_{1,4} = 6.12$, $p = .069$). When the number of object categories and trials were matched between the two experiments, weaker but similar results were obtained in both the LO and inferior IPS (shape by experiment interaction, $Fs > 4.91$, $ps < .09$; and location by experiment interaction, $Fs > 7.13$, $ps < .056$). Overall, these results show that, in the LO and inferior IPS, shape and location features are represented more strongly when the task engages shape processing and hence more attention to the object. This was true for both the task-relevant feature (shape) and the task-irrelevant feature (location). When attention was engaged in neither shape nor location processing, these features were still encoded robustly despite the fact that their encodings were completely task irrelevant and unnecessary.

In Experiment 2, in LO, decoding difference between shoes and bikes and between guitars and couches was not significant ($Fs < 1$, $ps > .67$). In inferior IPS, decoding between guitars and couches was better than decoding between shoes and bikes ($F_{1,4} = 11.31$, $p = .028$), with no other main effect or interactions ($Fs < 1.5$, $ps > .28$). It thus seems that differences between guitars and couches were better represented than those between shoes and bikes in inferior IPS. However, because this difference was not found in superior IPS (see previous results), the lack of shape encoding in superior IPS in the motion task could not therefore be attributed to the specific shape categories used, but must indicate a general lack of shape encoding in this brain area when shape information was task irrelevant.

DISCUSSION

Using fMRI MVPA and a VSTM task, we found that the human superior IPS represents object shape information in a task-dependent manner. Specifically, shape representation was present when it was required by a task and absent when it was task irrelevant. In other words, the nature of the task has a strong influence on the nature of object representation in superior IPS. This is consistent with results obtained in fMRI response amplitude measures in which superior IPS was found to track the encoding of task-relevant items in VSTM (Todd & Marois, 2004; Xu & Chun, 2006) and ignore task irrelevant object features or distractors (Jeong & Xu, 2013; Xu, 2010). Thus, shape representation in superior IPS is dynamic and task driven, similar to responses observed in LIP neurons in monkey neurophysiology studies (Fitzgerald, Swaminathan, & Freedman, 2012; Freedman & Assad, 2006, 2009; Swaminathan & Freedman, 2012; Toth & Assad, 2002). Although the exact human homologue of LIP is still under debate, our results suggest possible functional correspondence between the human superior IPS and monkey LIP.

Human parietal cortex has been implicated in attention-related processing (Corbetta & Shulman, 2002; Szczepanski et al., 2010; Wojciulik & Kanwisher, 1999; Yantis et al., 2002) and has the capability of directing encoding resources in posterior sensory regions. By showing the encoding of visual information in a task-dependent manner in superior IPS, the present finding puts forward an alternative, perhaps equally important, mechanism by which parietal attention control mechanism can exert its influence on visual information processing in the brain. By directly encoding task-relevant visual information, superior IPS functions similarly as the random access memory in a computer in which information important for the current task and goal is gathered and possibly integrated.

Although task also enhanced shape representation in other regions such as inferior IPS and LO, this enhancement was not specific to the task-relevant feature as it also boosted the encoding of a task-irrelevant feature. Moreover, shape representation persisted even when it was task irrelevant. This is qualitatively different from what was observed in superior IPS in which without a shape-task, shape representation was absent. Thus, task and attention may play two primary roles during visual information transmission: Modulating but without altering what is intrinsically represented in a brain region, such as those in LO and inferior IPS; or determining the nature of representation in a brain region, such as that in superior IPS.

Previous fMRI studies have reported attentional modulation of visual information representation in human parietal cortex (Liu, Hospadaruk, Zhu, & Gardner, 2011; Thompson & Duncan, 2009; Woolgar, Hampshire, Thompson, & Duncan, 2011). By either treating parietal cortex as a single functionally uniform region or failing to find distinctions among topographically defined subregions within parietal cortex, these studies either assumed or argued for functional homogeneity of the human parietal cortex. However, using a functionally defined ROI-based approach, here we show distinctive response profiles from inferior and superior IPS and illustrate different ways in which attention could influence visual information processing. Thus, with appropriate localizers, functionally heterogeneous brain regions can be unveiled in human parietal cortex, providing us with a richer understanding of the precise and unique roles of parietal cortex in visual cognition.

Functional heterogeneity in IPS regions may also explain inconsistencies across published studies. Although some recent studies have found successful decoding of VSTM contents in IPS (Christophel & Haynes, 2014; Christophel, Hebart, & Haynes, 2012), some failed to do so (Emrich, Riggall, Larocque, & Postle, 2013; Linden, Oosterhof, Klein, & Downing, 2012; Riggall & Postle, 2012). It is possible that these studies examined different IPS regions, and depending on whether or not the superior IPS was included, the decoding results varied. In the current study, we functionally localized voxels within the IPS that tracked VSTM capacity in individual observers and found decoding of task relevant visual information in the superior IPS. Studies using a searchlight approach to locate informative voxels have also reported decoding of VSTM representation in the parietal cortex (Christophel et al., 2012; Christophel & Haynes, 2014). It thus seems that methods using an information-based approach have all showed the involvement of parietal cortex in VSTM representation. Beyond functional heterogeneity in parietal cortex, factors such as the stimuli used may also contribute to whether or not VSTM contents may be decoded from IPS. It seems that studies using motion stimuli have not found VSTM decoding in parietal cortex (Emrich et al., 2013; Riggall & Postle, 2012), whereas studies using nonmotion stimuli have (Christophel et al., 2012; Christophel & Haynes, 2014). This suggests that distinct neural mechanisms may exist for VSTM representations of motion and nonmotion stimuli.

In sum, our findings show that the human parietal cortex plays a greater role than simply directing attentional resources during visual perception. A subregion in human parietal cortex, the superior IPS, is capable of directly representing incoming visual information in a task-dependent manner. This is consistent with a growing body of evidence suggesting that the human parietal cortex is part of a brain network involved in the flexible and dynamic representation and processing of incoming information (Cole et al., 2013; Cusack & Owen, 2008; Emrich, Burianová,

& Ferber, 2011; Fedorenko, Duncan, & Kanwisher, 2013; Vincent, Kahn, Snyder, Raichle, & Buckner, 2008). We would like to argue that the superior IPS may be a key node in this network that mediates the moment-to-moment, goal-directed visual information representation in the human brain.

Acknowledgments

This research was supported by NSF grant 0855112 and NIH grant 1R01EY022355 to Y.X.

References

Alvarez, G. A., & Cavanagh, P. (2004). The capacity of visual short-term memory is set both by visual information load and by number of objects. *Psychological Science*, *15*(2), 106–111.

Bahrami, B. (2003). Object property encoding and change blindness in multiple object tracking. *Visual Cognition*, *10*(8), 949–963. http://dx.doi.org/10.1080/13506280344000158.

Bays, P. M., & Husain, M. (2008). Dynamic shifts of limited working memory resources in human vision. *Science*, *321*(5890), 851–854. http://dx.doi.org/10.1126/science.1158023 (New York, N.Y.).

Brainard, D. H. (1997). The psychophysics toolbox. *Spatial Vision*, *10*(4), 433–436.

Christophel, T. B., & Haynes, J.-D. (2014). Decoding complex flow-field patterns in visual working memory. *NeuroImage*, *91*, 43–51. http://dx.doi.org/10.1016/j.neuroimage.2014.01.025.

Christophel, T. B., Hebart, M. N., & Haynes, J.-D. (2012). Decoding the contents of visual short-term memory from human visual and parietal cortex. *The Journal of Neuroscience: The Official Journal of the Society for Neuroscience*, *32*(38), 12983–12989. http://dx.doi.org/10.1523/JNEUROSCI.0184-12.2012.

Cole, M. W., Reynolds, J. R., Power, J. D., Repovs, G., Anticevic, A., & Braver, T. S. (2013). Multi-task connectivity reveals flexible hubs for adaptive task control. *Nature Neuroscience*, *16*(9), 1348–1355. http://dx.doi.org/10.1038/nn.3470.

Corbetta, M., & Shulman, G. L. (2002). Control of goal-directed and stimulus-driven attention in the brain. *Nature Reviews. Neuroscience*, *3*(3), 201–215. http://dx.doi.org/10.1038/nrn755.

Coslett, H. B., & Saffran, E. (1991). Simultanagnosia. To see but not two see. *Brain: A Journal of Neurology*, *114*(Pt 4), 1523–1545.

Cowan, N. (2001). The magical number 4 in short-term memory: a reconsideration of mental storage capacity. *The Behavioral and Brain Sciences*, *24*(1), 87–114; discussion 114–185.

Cox, D. D., & Savoy, R. L. (2003). Functional magnetic resonance imaging (fMRI) "brain reading": detecting and classifying distributed patterns of fMRI activity in human visual cortex. *NeuroImage*, *19*(2 Pt 1), 261–270.

Cusack, R., & Owen, A. M. (2008). Distinct networks of connectivity for parietal but not frontal regions identified with a novel alternative to the "resting state" method. *Proceedings of Cognitive Neuroscience Society*, 1.

Emrich, S. M., Burianová, H., & Ferber, S. (2011). Transient perceptual neglect: visual working memory load affects conscious object processing. *Journal of Cognitive Neuroscience*, *23*(10), 2968–2982. http://dx.doi.org/10.1162/jocn_a_00028.

Emrich, S. M., Riggall, A. C., Larocque, J. J., & Postle, B. R. (2013). Distributed patterns of activity in sensory cortex reflect the precision of multiple items maintained in visual short-term memory. *Journal of Neuroscience*, *33*(15), 6516–6523. http://dx.doi.org/10.1523/JNEUROSCI.5732-12.2013.

Fedorenko, E., Duncan, J., & Kanwisher, N. G. (2013). Broad domain generality in focal regions of frontal and parietal cortex. *Proceedings of the National Academy of Sciences of the United States of America*, *110*(41), 16616–16621. http://dx.doi.org/10.1073/pnas.1315235110.

Fitzgerald, J. K., Swaminathan, S. K., & Freedman, D. J. (2012). Visual categorization and the parietal cortex. *Frontiers in Integrative Neuroscience*, *6*, 18. http://dx.doi.org/10.3389/fnint.2012.00018.

Freedman, D. J., & Assad, J. A. (2006). Experience-dependent representation of visual categories in parietal cortex. *Nature*, *443*(7107), 85–88. http://dx.doi.org/10.1038/nature05078.

Freedman, D. J., & Assad, J. A. (2009). Distinct encoding of spatial and nonspatial visual information in parietal cortex. *The Journal of Neuroscience: the Official Journal of the Society for Neuroscience*, *29*(17), 5671–5680. http://dx.doi.org/10.1523/JNEUROSCI.2878-08.2009.

Garrido, L., Vaziri-Pashkam, M., Nakayama, K., & Wilmer, J. (2013). The consequences of subtracting the mean pattern in fMRI multivariate correlation analyses. *Frontiers in Neuroscience*, *7*, 174. http://dx.doi.org/10.3389/fnins.2013.00174.

Gottlieb, J. P., Kusunoki, M., & Goldberg, M. E. (1998). The representation of visual salience in monkey parietal cortex. *Nature*, *391*(6666), 481–484. http://dx.doi.org/10.1038/35135.

Grill-Spector, K., Kushnir, T., Hendler, T., & Malach, R. (2000). The dynamics of object-selective activation correlate with recognition performance in humans. *Nature Neuroscience*, *3*(8), 837–843. http://dx.doi.org/10.1038/77754.

Harrison, S. A., & Tong, F. (2009). Decoding reveals the contents of visual working memory in early visual areas. *Nature*, *458*(7238), 632–635. http://dx.doi.org/10.1038/nature07832.

Haxby, J. V., Gobbini, M. I., Furey, M. L., Ishai, A., Schouten, J. L., & Pietrini, P. (2001). Distributed and overlapping representations of faces and objects in ventral temporal cortex. *Science*, *293*(5539), 2425–2430. http://dx.doi.org/10.1126/science.1063736 (New York, N.Y.).

Haynes, J.-D., & Rees, G. (2006). Decoding mental states from brain activity in humans. *Nature Reviews. Neuroscience*, *7*(7), 523–534. http://dx.doi.org/10.1038/nrn1931.

Huettel, S. A., Song, A. W., & McCarthy, G. (2009). *Functional magnetic resonance imaging* (2nd ed.). Sunderland, MA: Sinauer Associates.

Jeong, S. K., & Xu, Y. (2013). Neural representation of Targets and distractors during object individuation and identification. *Journal of Cognitive Neuroscience*, *25*(1), 117–126. http://dx.doi.org/10.1162/jocn_a_00298.

Kravitz, D. J., Kriegeskorte, N., & Baker, C. I. (2010). High-level visual object representations are constrained by position. *Cerebral Cortex*, *20*(12), 2916–2925. http://dx.doi.org/10.1093/cercor/bhq042 (New York, N.Y.: 1991).

Leslie, A. M., Xu, F., Tremoulet, P. D., & Scholl, B. J. (1998). Indexing and the object concept: developing 'what' and 'where' systems. *Trends in Cognitive Sciences*, *2*(1), 10–18.

Linden, D. E. J., Oosterhof, N. N., Klein, C., & Downing, P. E. (2012). Mapping brain activation and information during category-specific visual working memory. *Journal of Neurophysiology*, *107*(2), 628–639. http://dx.doi.org/10.1152/jn.00105.2011.

Liu, T., Hospadaruk, L., Zhu, D. C., & Gardner, J. L. (2011). Feature-specific attentional priority signals in human cortex. *The Journal of Neuroscience: The Official Journal of the Society for Neuroscience*, *31*(12), 4484–4495. http://dx.doi.org/10.1523/JNEUROSCI.5745-10.2011.

Luck, S. J., & Vogel, E. K. (1997). The capacity of visual working memory for features and conjunctions. *Nature*, *390*(6657), 279–281. http://dx.doi.org/10.1038/36846.

Milner, A. D., Perrett, D. I., Johnston, R. S., Benson, P. J., Jordan, T. R., Heeley, D. W., et al. (1991). Perception and action in 'visual form agnosia'. *Brain: A Journal of Neurology*, *114*(Pt 1B), 405–428.

Norman, K. A., Polyn, S. M., Detre, G. J., & Haxby, J. V. (2006). Beyond mind-reading: multi-voxel pattern analysis of fMRI data. *Trends in Cognitive Sciences*, *10*(9), 424–430. http://dx.doi.org/10.1016/j.tics.2006.07.005.

Pashler, H. (1988). Familiarity and visual change detection. *Perception & Psychophysics*, *44*(4), 369–378.

Peelen, M. V., & Downing, P. E. (2007). Using multi-voxel pattern analysis of fMRI data to interpret overlapping functional activations. *Trends in Cognitive Sciences*, *11*(1), 4–5. http://dx.doi.org/10.1016/j.tics.2006.10.009.

Phillips, W. A. (1974). On the distinction between sensory storage and short-term visual memory. *Perception & Psychophysics*, *16*, 283–290.

Riggall, A. C., & Postle, B. R. (2012). The relationship between working memory storage and elevated activity as measured with functional magnetic resonance imaging. *The Journal of Neuroscience: The Official Journal of the Society for Neuroscience*, *32*(38), 12990–12998. http://dx.doi.org/10.1523/JNEUROSCI.1892-12.2012.

Schwarzlose, R. F., Swisher, J. D., Dang, S., & Kanwisher, N. G. (2008). The distribution of category and location information across object-selective regions in human visual cortex. *Proceedings of the National Academy of Sciences of the United States of America*, *105*(11), 4447–4452. http://dx.doi.org/10.1073/pnas.0800431105.

Swaminathan, S. K., & Freedman, D. J. (2012). Preferential encoding of visual categories in parietal cortex compared with prefrontal cortex. *Nature Neuroscience*, *15*(2), 315–320. http://dx.doi.org/10.1038/nn.3016.

Szczepanski, S. M., Konen, C. S., & Kastner, S. (2010). Mechanisms of spatial attention control in frontal and parietal cortex. *The Journal of Neuroscience: The Official Journal of the Society for Neuroscience*, *30*(1), 148–160. http://dx.doi.org/10.1523/JNEUROSCI.3862-09.2010.

Thompson, R., & Duncan, J. (2009). Attentional modulation of stimulus representation in human fronto-parietal cortex. *NeuroImage*, *48*(2), 436–448. http://dx.doi.org/10.1016/j.neuroimage.2009.06.066.

Todd, J. J., & Marois, R. (2004). Capacity limit of visual short-term memory in human posterior parietal cortex. *Nature*, *428*(6984), 751–754. http://dx.doi.org/10.1038/nature02466.

Todd, J. J., & Marois, R. (2005). Posterior parietal cortex activity predicts individual differences in visual short-term memory capacity. *Cognitive, Affective & Behavioral Neuroscience*, *5*(2), 144–155.

Toth, L. J., & Assad, J. A. (2002). Dynamic coding of behaviourally relevant stimuli in parietal cortex. *Nature*, *415*(6868), 165–168. http://dx.doi.org/10.1038/415165a.

van den Berg, R., Shin, H., Chou, W.-C., George, R., & Ma, W. J. (2012). Variability in encoding precision accounts for visual short-term memory limitations. *Proceedings of the National Academy of Sciences of the United States of America*, *109*(22), 8780–8785. http://dx.doi.org/10.1073/pnas.1117465109.

Vincent, J. L., Kahn, I., Snyder, A. Z., Raichle, M. E., & Buckner, R. L. (2008). Evidence for a frontoparietal control system revealed by Intrinsic functional connectivity. *Journal of Neurophysiology*, *100*(6), 3328–3342. http://dx.doi.org/10.1152/jn.90355.2008.

Vogel, E. K., & Machizawa, M. G. (2004). Neural activity predicts individual differences in visual working memory capacity. *Nature*, *428*(6984), 748–751. http://dx.doi.org/10.1038/nature02447.

Vogel, E. K., Woodman, G. F., & Luck, S. J. (2001). Storage of features, conjunctions and objects in visual working memory. *Journal of Experimental Psychology. Human Perception and Performance*, *27*(1), 92–114.

Wilken, P., & Ma, W. J. (2004). A detection theory account of change detection. *Journal of Vision*, *4*(12), 1120–1135. http://dx.doi.org/10.1167/4.12.11.

Williams, M. A., Dang, S., & Kanwisher, N. G. (2007). Only some spatial patterns of fMRI response are read out in task performance. *Nature Neuroscience*, *10*(6), 685–686. http://dx.doi.org/10.1038/nn1900.

Wilson, K. E., Adamo, M., Barense, M. D., & Ferber, S. (2012). To bind or not to bind: addressing the question of object representation in visual short-term memory. *Journal of Vision*, *12*(8), 14. http://dx.doi.org/10.1167/12.8.14.

Wojciulik, E., & Kanwisher, N. G. (1999). The generality of parietal involvement in visual attention. *Neuron*, *23*(4), 747–764.

Woolgar, A., Hampshire, A., Thompson, R., & Duncan, J. (2011). Adaptive coding of task-relevant information in human frontoparietal cortex. *The Journal of Neuroscience: The Official Journal of the Society for Neuroscience*, *31*(41), 14592–14599. http://dx.doi.org/10.1523/JNEUROSCI.2616-11.2011.

Xu, Y. (2002). Encoding color and shape from different parts of an object in visual short-term memory. *Perception & Psychophysics*, *64*(8), 1260–1280.

Xu, Y. (2007). The role of the superior intraparietal sulcus in supporting visual short-term memory for multifeature objects. *The Journal of Neuroscience: The Official Journal of the Society for Neuroscience*, *27*(43), 11676–11686. http://dx.doi.org/10.1523/JNEUROSCI.3545-07.2007.

Xu, Y. (2008). Representing connected and disconnected shapes in human inferior intraparietal sulcus. *NeuroImage*, *40*(4), 1849–1856. http://dx.doi.org/10.1016/j.neuroimage.2008.02.014.

Xu, Y. (2009). Distinctive neural mechanisms supporting visual object individuation and identification. *Journal of Cognitive Neuroscience*, *21*(3), 511–518. http://dx.doi.org/10.1162/jocn.2008.21024.

Xu, Y. (2010). The neural fate of task-irrelevant features in object-based processing. *The Journal of Neuroscience: The Official Journal of the Society for Neuroscience*, *30*(42), 14020–14028. http://dx.doi.org/10.1523/JNEUROSCI.3011-10.2010.

Xu, Y., & Chun, M. M. (2006). Dissociable neural mechanisms supporting visual short-term memory for objects. *Nature*, *440*(7080), 91–95. http://dx.doi.org/10.1038/nature04262.

Xu, Y., & Chun, M. M. (2007). Visual grouping in human parietal cortex. *Proceedings of the National Academy of Sciences of the United States of America*, *104*(47), 18766–18771. http://dx.doi.org/10.1073/pnas.0705618104.

Xu, Y., & Chun, M. M. (2009). Selecting and perceiving multiple visual objects. *Trends in Cognitive Sciences*, *13*(4), 167–174. http://dx.doi.org/10.1016/j.tics.2009.01.008.

Yantis, S., Schwarzbach, J., Serences, J. T., Carlson, R. L., Steinmetz, M. A., Pekar, J. J., et al. (2002). Transient neural activity in human parietal cortex during spatial attention shifts. *Nature Neuroscience*, *5*(10), 995–1002. http://dx.doi.org/10.1038/nn921.

Zhang, W., & Luck, S. J. (2008). Discrete fixed-resolution representations in visual working memory. *Nature*, *453*(7192), 233–235. http://dx.doi.org/10.1038/nature06860.